Radio-Wave Propagation Into Large Building Structures—Part 2: Characterization of Multipath

Kate A. Remley, *Senior Member, IEEE*, Galen Koepke, *Member, IEEE*, Christopher L. Holloway, *Fellow, IEEE*, Chriss A. Grosvenor, *Member, IEEE*, Dennis Camell, *Member, IEEE*, John Ladbury, *Member, IEEE*, Robert T. Johnk, *Member, IEEE*, and William F. Young, *Member, IEEE*

***Abstract*—We report on measurements that characterize multipath conditions that affect broadband wireless communications in building penetration scenarios. Measurements carried out in various large structures quantify both radio-signal attenuation and distortion (multipath) in the radio propagation channel. Our study includes measurements of the complex, wideband channel transfer function and bandpass measurements of a 20 MHz-wide, digitally modulated signal. From these, we derive the more compact metrics of time delay spread, total received power and error vector magnitude that summarize channel characteristics with a single number. We describe the experimental set-up and the measurement results for data collected in representative structures. Finally, we discuss how the combination of propagation metrics may be used to classify different propagation channel types appropriate for public-safety applications.**

***Index Terms*—Attenuation, broadband radio communications, building penetration, digital modulation, emergency responders, error vector magnitude, excess path loss, received power, time-delay spread, vector network analyzer, vector signal analyzer, wireless signals, wireless system measurements, wireless telecommunications.**

I. Introduction

To aid in the development of standards that support reliable wireless communications for emergency responders such as those discussed in [1], the National Institute of Standards and Technology (NIST) has embarked on a project to acquire data on radio-wave propagation in key emergency-responder and public-safety environments. In past work [2]–[4], measurements were made in buildings scheduled for implosion to simulate collapsed-building environments. The focus of current work [5], [6] is to study the penetration of radio waves into large buildings where difficult radio reception is often encountered because of signal attenuation and variability. Our measurement set-up is intended to simulate a response scenario, where an incident command vehicle is located near a structure and a mobile unit is deployed inside. In contrast to the many existing studies on cell- or trunked-radio systems, in our case we focus on ground-based point-to-point radio communications.

Our goal is to provide a large body of measurement data, acquired in key responder environments, to the open literature (see [7] for a complete list) for improved communication system development and design and to aid in technically sound standards development. A second goal is to share our methodology so that responder organizations and others may carry out these characterizations as desired. A third goal of this program is to provide measurement data that will be useful for verification of network simulations of emergency responder radio links. Such simulations are being developed by NIST, among others [8].

Much work has been published describing measurement characterization of multipath in the radio-propagation environment. Various figures of merit are often used to describe multipath effects, including excess path loss, frequency selectivity, time delay spread, bit error rate (BER) and its variants, and/or error vector magnitude (EVM). Most of these publications (for example, [9]–[13] and references cited therein) describe measurements intended to simulate communications via cellular telephone or other wireless systems that rely on a fixed base station whose antenna is positioned high above the ground and a mobile user located at ground level. Only a few publications describe measurements that simulate point-to-point radio-communication scenarios, such as those utilized in many emergency-responder scenarios. Examples include sections of [10], [14] and references cited therein, and [15].

Part 1 of this work [16] summarizes the statistics of received-signal-strength measurements under single-frequency excitation in twelve large public building structures, based on NIST Technical Note 1545 [5]. In that work, a spectrum analyzer was used to measure the relative received signal strength at a fixed receiver location as a portable transmitter was carried throughout the buildings. The mean and standard deviation of the measurements in the structures were calculated. Frequencies included bands near licensed public-safety bands and cell phone bands including 49 MHz, 160 MHz, 225 MHz, 450 MHz, 900 MHz, 1.8 GHz, and a limited set of data at 2.4 GHz and 4.95 GHz.

In this paper, we focus on additional parameters relevant to successful transmission of modulated signals including wideband channel frequency response, excess path loss, time delay spread, channel power and error vector magnitude. We focus on

Manuscript received December 18, 2008; revised August 10, 2009; accepted September 25, 2009. Date of publication January 22, 2010; date of current version April 07, 2010. This work was supported in part by the U.S. Department of Justice, Community-Oriented Police Services through the NIST Public-Safety Communications Research Laboratory.

K. A. Remley, G. Koepke, C. L. Holloway, C. Grosvenor, D. Camell, J. Ladbury, and W. F. Young are with the National Institute of Standards and Technology, Boulder, CO 80305 USA (e-mail: remley@boulder.nist.gov; kate.remley@nist.gov; koepke@boulder.nist.gov; holloway@boulder.nist.gov; chriss@boulder.nist.gov; camell@boulder.nist.gov; ladbury@boulder.nist.gov; wfyoung@sandia.gov).

R. T. Johnk was with the National Institute of Standards and Technology, Boulder, CO 80305 USA. He is now with the Institute for Telecommunication Sciences, Boulder, CO 80305 USA (e-mail: bjohnk@its.bldrdoc.gov).

Color versions of one or more of the figures in this paper are available online at http://ieeexplore.ieee.org.

Digital Object Identifier 10.1109/TAP.2010.2041143

carrier frequencies over 1 GHz, focusing on frequency bands around 2.4 GHz and 4.95 GHz to investigate the differences in transmission between existing wireless systems in the unlicensed 2.4 GHz industrial/scientific/medical (ISM) frequency band (which is sometimes used by public-safety organizations) and systems proposed for use in the licensed public-safety frequency band covering 4.94 GHz to 4.99 GHz [17], [18].

In NIST Technical Note 1546 [6], we conducted tests in four representative environments that are notoriously difficult in terms of radio reception for emergency responders. These are a multi-story apartment building, an oil refinery, a long corridor in an office building typical of many commercial facilities, and a subterranean tunnel. Here we provide representative results of the characterization of multipath in the propagation channel and discuss key findings from [6].

We extend the work of [6] to demonstrate how compact "summary" metrics that quantify the channel characteristics with a single number, may be used to classify propagation channels for responder applications. Summary metrics are often easier and more inexpensive to acquire than are extensive frequency-domain measurements. By classifying propagation channel types, responders may better know how to deploy wireless systems, and standards development organizations may develop better performance metrics and verification tests for wireless technology. These data may also be used to support general building or scenario classifications such as those presented in [9], [10].

In Section II, we discuss the instrumentation, calibrations, and post-processing methods we used to collect the various data. In Section III, we show representative measured data collected at two of the four large structures reported in [5], [6]: an 11-story apartment building and an oil refinery. We summarize the propagation effects that we observed and draw some conclusions on the characteristics of the propagation channels seen in the structures.

Occasionally product names are specified solely for completeness of description, but such identification constitutes no endorsement by the National Institute of Standards and Technology. Other products may work as well or better.

II. Measurements for Modulated-Signal Channel Characterization

A. Overview

In the study of [6], we conducted three types of measurements: single-frequency received-power using a communications receiver; frequency response data over a very broad frequency band at fixed points in the propagation environment using a vector network analyzer (VNA); and modulated-signal measurements using a vector signal analyzer (VSA). The single-frequency data are similar to those reported in [5] and are not discussed here. From the VNA data, we determined the wideband frequency response of the propagation channel and, from this, the excess path loss (the loss that exceeds that measured in a free-space environment [19], [20]). After transforming these data to the time domain, we calculated the root-mean-square (RMS) time-delay spread. The RMS delay spread is a figure of merit that quantifies the time it takes for reflections in a received signal to die out. Using the VSA, we also collected modulated-signal measurements associated with broadband digitally modulated signals at 2.4 GHz and 4.95 GHz. From these, we found the error vector magnitude (EVM) in each environment. EVM is a figure of merit that describes the level of distortion in received, demodulated symbols of a digitally modulated signal. In the following sections, we describe these measurements.

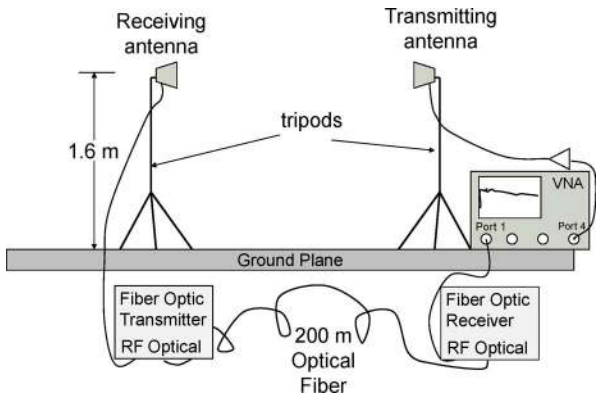

Fig. 1. Wideband measurement system based on a vector network analyzer. Frequency-domain measurements, synchronized by the optical fiber link, are transformed to the time domain in post-processing. This enables determination of excess path loss, time-delay spread, and other figures of merit important in characterizing broadband modulated-signal transmissions.

B. Wideband Vector Network Analyzer Measurements

1) Measurement Set-Up: We measured the wideband frequency response and time-delay characteristics of the propagation channel using a measurement system based on a vector network analyzer, shown in Fig. 1. This instrument collects data over a very wide frequency range, from 25 MHz to 18 GHz for the system we used. This system, also described in [19], lets us measure the complex transfer function of the channel, including frequency-selective characteristics. By taking the inverse Fourier transform of the measured transfer function, the power delay profile and RMS delay spread of the channel are found in post processing.

The VNA acts as both transmitter and receiver in this system. The transmitting section of the VNA steps through the frequencies a single frequency at a time. The signal is amplified and fed to a transmitting antenna, as shown in Fig. 1. The received signal is returned to the VNA via a fiber-optic cable. Transmitting the received signal along the fiber optic cable back to the VNA eliminates the loss and phase changes that would be associated with RF coaxial cables between the receive antenna and the transmit antenna, allowing characterization of the complex radio channel. One advantage of this system is that it provides a high dynamic range relative to true time-domain-based measurement instruments.

In Fig. 1, the system is configured for a line-of-sight reference measurement. In practice, the transmitting and receiving antennas may be separated by significant distances, although they must remain tethered together by the fiber-optic link. While directional horn antennas are shown in Fig. 1, omnidirectional antennas were also used in our measurements. Omnidirectional antennas are most often used in public-safety applications. However, high-frequency measurements often benefit from the use of directional antennas to maximize gain in a specific direction.

Emergency response agencies may use directional antennas in these situations as well.

We made measurements in two frequency bands: a low band that ranged from 100 MHz to 1.2 GHz, and a high band, that ranged from 1 GHz to 18 GHz. We used omnidirectional transmit and receive antennas for the lower frequency band and, for the measurements reported on here, a dual-ridge-guide (DRG) directional transmit antenna and omnidirectional receive antenna for the higher frequency band (1 GHz to 18 GHz). The beamwidth of the omnidirectional antennas is approximately 40° to 50° in the vertical direction. The beamwidth of the DRG varies with frequency, from almost $\pm 45°$ at the low end at about 1 GHz to $\pm 20°$ at 18 GHz, necessitating reorientation of the antenna to track the receiver's position in certain structures such as the apartment building.

It is well known that in propagation environments where the transmitting antenna is located in the midst of highly reflecting objects, the use of a directional horn antenna can reduce the apparent multipath by eliminating reflections from behind. Our studies in an automobile manufacturing plant [21] demonstrated this. For the measurements presented here, strong reflectors (the building structures) were located in front of the transmitting antenna with very few scatterers behind. Thus, we anticipate the use of directional antennas introduced only small deviations to the measured multipath effects.

To make a measurement, the vector network analyzer is first calibrated by use of standard techniques where known impedance standards are measured. The calibration enables us to correct for the response of the fiber-optic system, amplifiers, and any other passive elements and electronics used in the measurement. We also high-pass filter our measurements in post processing to suppress the large, low-frequency oscillation that occurs in the optical fiber link.

For the measurements reported here, the VNA-based measurement system was set up with the following parameters: the initial output power was set between -15 dBm to -13 dBm. The gain of the amplifier and the optical link and the system losses resulted in a received power level no more than 0 dBm. An intermediate-frequency (IF) averaging bandwidth of around 1 kHz was used to average the received signal. We typically recorded 6401 points per frequency band and chose the number of bands recorded in each measurement to avoid aliasing of the signal. We report here on our high-band measurements ranging from 1 GHz to 18 GHz, which were taken by measuring 48003 points for a total of three bands. Low-frequency measurements from 100 MHz to 1.2 GHz are reported in [6]. The dwell time was approximately 25 μs per point and the frequency spacing was approximately 379 kHz.

2) Wideband Frequency Response and Path Loss: Our wideband measurements provide a channel transfer function $H(f)$, where $H(f)$ typically is derived from the measured transmission parameter $S_{21}(f)$. To find the frequency-dependent path loss between the transmit and receive antennas, we first compute $|H(f)|^2/|H_{\rm r}(f)|^2$, where $H_{\rm r}(f)$ is a free-space reference made at a known distance $d_{\rm r}$ from the transmit antenna. The use of a ratio to find the path loss enables us to calibrate out the antenna response of the system. We correct the measurements for the free-space path loss between the transmit antenna and the reference location by dividing $|H_{\rm r}(f)|^2$ by $(4\pi d_{\rm r}/\lambda)^2$.

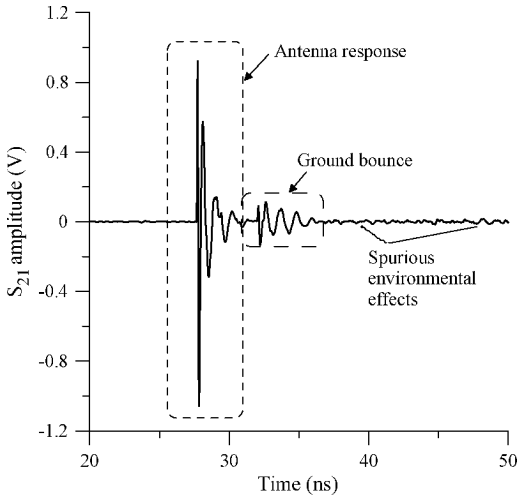

Fig. 2. Reference measurement at three meters for a dual-ridge guide horn antenna, transformed to the time domain. The waveform shows the antenna response, the ground-bounce response and the spurious environmental effects.

To find the excess path loss, we additionally reduce the total path loss by the expected free-space path loss over the overall separation distance d between the transmit and receive antennas. To do this, we divide the measurement of $|H(f)|^2$ by $(4\pi d/\lambda)^2$. Equivalently, we can multiply $|H(f)|^2/|H_{\rm r}(f)|^2$ by $(d_{\rm R}/d)^2$. The distance d may be measured or estimated from maps, depending on the environment. As stated earlier, this provides the loss in excess of that which would be measured at the same distance in free space. We note that communication engineers typically think of excess path loss as a single frequency or narrowband measurement. However, the VNA measurements provide a much richer data set because they include both magnitude and phase information over a broad frequency range.

The reference measurement is made at a specified distance and may be acquired either during field tests or from a laboratory measurement. In the field, the measurement includes environmental effects, and we use time-domain gating to minimize reflections on the free-space reference. If we are not able to gate out the reflections satisfactorily, the reference measurement is made in a laboratory facility such as an anechoic chamber or an open-area test site. In this case, we use the same antennas and measurement system as were used in the field. For the measurements shown below, we used a two-meter reference made in the field. We chose this distance to balance the need to be in the antenna far field of our lowest frequency of interest (1 GHz for the results reported here), while keeping the reference measurement as free from environmental reflections as possible.

As an example, Fig. 2 shows the time-domain response for a reference measurement using a pair of dual-ridged-guide antennas separated by 3 m. In Fig. 2, the reference measurement, transformed to the time domain, is shown with all environmental effects. The reference measurement is gated (windowed) from 20 ns to 32 ns to isolate the antenna response, which was determined previously in a separate measurement. The frequency-domain responses for the reference measurement would show

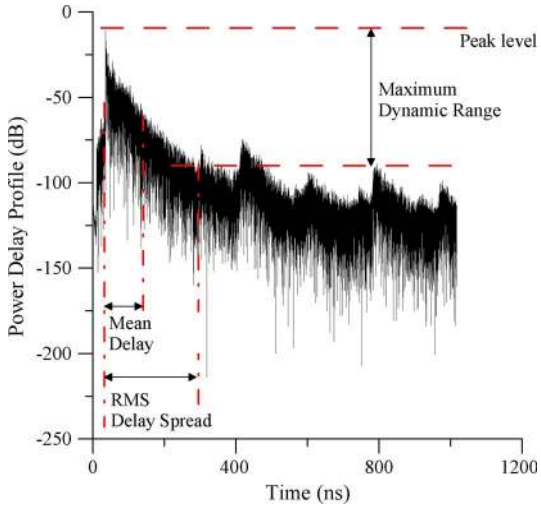

Fig. 3. Power-delay profile for a building propagation measurement. Important parameters for a measured signal are the peak level, the maximum dynamic range, the mean delay, and the RMS delay spread.

a noisier trace when environmental effects are included, compared with a smoother trace for isolated antennas. The gated response is what we would see if the antenna were measured in a free-space environment, free from environmental reflections.

In the following, we present graphs of the inverse excess path loss in decibels. Graphs of path loss would have positive ordinates and increase with distance. Thus, we refer to the curves in our graphs as "penetration." This terminology is commonly used in studies of electromagnetic shielding.

3) RMS Delay Spread: The time-domain representation of the signal was calculated from the excess path loss data in post processing. From this we found the RMS delay spread. RMS delay spread is calculated as the square root of the second central moment of the power-delay profile of a measured signal [22]–[24]. Fig. 3 shows the power-delay profile for a representative building propagation measurement. The peak level usually occurs when the signal first arrives at the receiving antenna, although in high multipath environments we sometimes see the signal build up over time to a peak value and then fall off.

A common rule of thumb is to calculate the RMS delay spread from signals at least 10 dB above the noise floor of the measurement [24]. For the measurements described in the following sections, we defined the minimum dynamic range to be approximately 40 dB below the peak value, although this value was reduced for lower signal levels. For the illustrative measurement shown in Fig. 3, we extended the window down to 70 dB below the peak value. Whether we use a 40 dB or a 70 dB threshold, the RMS delay spread does not change appreciably due to the almost constant slope of the power decay curve.

The RMS delay spread σ_{T} can be defined as

$$\sigma_\tau = \sqrt{\overline{\tau^2} - (\overline{\tau})^2}. \tag{1}$$

In (1), $\overline{\tau}$ is defined as the average value of the power-delay profile in the defined dynamic range window, and $\overline{\tau^2}$ is the variance of the power-delay profile within this window.

C. Modulated-Signal Measurements

Along with the single-frequency measurements described in [5], [6] and the wideband VNA measurements described above, a third set of tests involved measuring the waveforms of digitally modulated signals. From these, we plotted the spectra of the signals, and calculated the received power and the error vector magnitude associated with a given propagation channel. EVM gives an indication of the distortion introduced into a digitally modulated signal as it passes through a propagation channel. Mathematically, this can be expressed as

$$EVM_{\mathrm{RMS}} = \left[\frac{\frac{1}{N}\sum_{r=1}^{N} |S_{\mathrm{ideal},r} - S_{\mathrm{meas},r}|^2}{\frac{1}{N}\sum_{r=1}^{N} |S_{\mathrm{ideal},r}|^2} \right]^{\frac{1}{2}} \tag{2}$$

where $S_{\mathrm{meas,r}}$ is the normalized r^{th} symbol in a stream of measured symbols, $S_{\mathrm{ideal,r}}$ is the ideal normalized constellation point for the r^{th} symbol, and N is the number of unique symbols in the constellation. The fractional form of EVM given in (2) is often represented as a percentage. The algorithm used to find EVM was built into the receiver.

The modulated signal used as excitation was based on orthogonal frequency-division multiplexing (OFDM) 802.11a/g, as specified by the IEEE 802.11a-1999 standard [25]–[27]. OFDM is used in wireless local-area networks (WLANs) and in the public-safety band at 4.95 GHz. In the latter, OFDM signals may be transmitted in a 10 MHz wide channel using the 802.11j standard, instead of the 20 MHz wide channel utilized in 802.11a. Our demodulator was able to measure only the 802.11a standard. As a consequence, this is what we report on in the following sections.

The OFDM multiplexing scheme was developed to provide immunity to interference. Data are encoded onto 52 narrowband, frequency-multiplexed subcarriers. For strong received signals, data are transmitted up to a maximum of 54 megabits per second (Mbps). As the received signal strength decreases or the level of multipath increases, the data rate decreases to compensate for the decrease in signal-to-noise ratio. In the tests reported here, we force the signal generator to transmit either a slow-data-rate quadrature-phase-shift-keyed (QPSK) or a high-data-rate 64-quadrature-amplitude-modulated (64QAM) signal. This lets us assess the impact of multipath for a given channel when different modulation schemes are used.

For the measurements described in the following sections, a vector signal generator was used to create the digitally modulated signals. The signal generator was mounted on a rolling cart and moved through the various propagation environments. We used omnidirectional antennas where possible to mimic those used by emergency responders. In some environments reported here, we were limited by the dynamic range of the receiver and so we used directional, dual-ridge-guide horn antennas.

We used a vector signal analyzer to acquire the signals. The VSA maintains the phase of the measured frequency components relative to one another and enables measurements of complex distortion in digitally modulated signals, including EVM. The VSA used had a 36 MHz measurement bandwidth. No correction for system effects such as antenna gain, system electronics, or system impedance mismatch was conducted. Thus,

these measurements are not absolute, but are relative to the measurement configuration we used. The VSA was adjusted for minimum received-signal distortion before each set of measurements. This entailed performing an internal calibration followed by a range adjustment under line-of-sight conditions.

III. Measurement Results and Identification of Channel Classifications

A. Overview

As stated in the introduction, in [6] we collected measurements in four large public structures, two of which are reported on here. By observing key features from graphs of the measurements, we are able to classify distinct propagation effects depending on the distance and type of structural obstruction between the transmitter and receiver. The propagation effects illustrated here are specifically relevant to point-to-point communications used by most emergency response organizations.

The primary features we observed to make our classifications include (*i*) the excess path loss, (*ii*) the amount and structure of frequency-selective distortion over the modulation bandwidth (in this case, the spectrum covering 2.4 GHz and 4.95 GHz $\pm$ 10 MHz), (*iii*) the RMS delay spread, (*iv*) the received channel power, and (*v*) the error vector magnitude. We illustrate how the summary metrics (*iii*)–(*v*) can be used to gain a similar insight into the channel as the more complete frequency-domain measurements (*i*) and (*ii*). We illustrate these concepts using measured results from an apartment building and an oil refinery. The latter was discussed in detail in [5] with respect to the use of single-frequency statistics to classify channels. The oil refinery was also discussed in [28] and [29] as part of overviews on the difficulties faced by public-safety practitioners and wireless sensor networks, respectively, in high-multipath environments. Here, we discuss how a combination of the metrics above can help to identify classes of propagation environments that may be important to the emergency response community. Again, the reader is referred to [6] for a more complete discussion.

B. Apartment Building

We carried out propagation measurements at an 11-story apartment building located in Boulder, Colorado in October 2007. The building, shown in Fig. 4, is constructed of reinforced concrete, steel, and brick. It contains standard interior finish materials. The building was fully furnished and occupied during the experiments. Measurements were performed during daytime hours, so people were moving throughout the building during the experiments.

The layout of each floor of the apartment building was T-shaped, with two elevators near the junction of the T. This is illustrated in Fig. 5. The hallway along top of the T was approximately 20 m long and the body of the T was approximately 50 meters long. Our receiver site was located approximately 60 m from the building in a parking lot, also shown in Fig. 5. Both VNA and VSA measurements were made every 5 meters, on Floors 2 and 7, as illustrated in Fig. 5.

This apartment building was chosen because it has several features in common with the building described in the Apartment Fire Scenario of the SAFECOM Statement of Requirements [1], including concrete construction, stairwells at the ends of the hallways, apartments off a main corridor with outside-facing windows, and the need for single- or two-wall radio-wave penetration. The Apartment Fire Scenario of [1] deals with a fire response on the second floor of such an apartment building.

Fig. 4. The 11-story, concrete, steel, and brick apartment building where the NIST measurements were made.

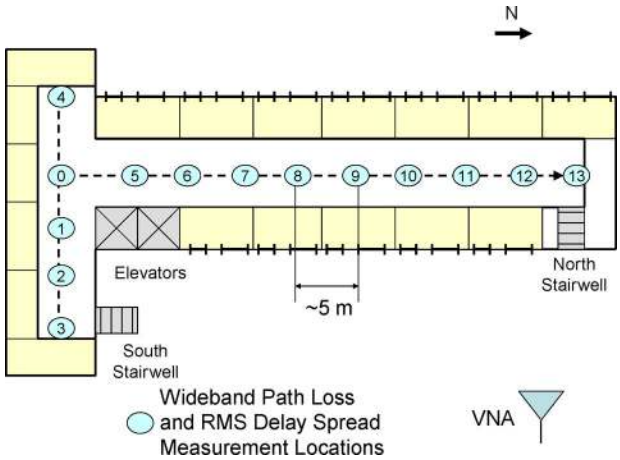

Fig. 5. Layout of a typical floor of the 11-story apartment building. Circles show the test positions where measurements were made. The receiver site shown is approximately 60 m east of the building.

The apartment building propagation environment consisted entirely of non-line-of-sight (NLOS) propagation paths because all of the received signals penetrated through the outside walls of the structure and at least one interior wall. The penetration measurement examples in Fig. 6 show a predominantly monotonic roll-off with frequency. These graphs show excess path loss from 1 GHz to 18 GHz made at test position 2 (Fig. 6(a)), where the only obstructions between transmitter and receiver are the building walls and windows, and test position 5 (Fig. 6(b)), where a metallic elevator obstructs the signal path.

The building penetration decreases with frequency indicating a channel that includes attenuation due to signal penetration

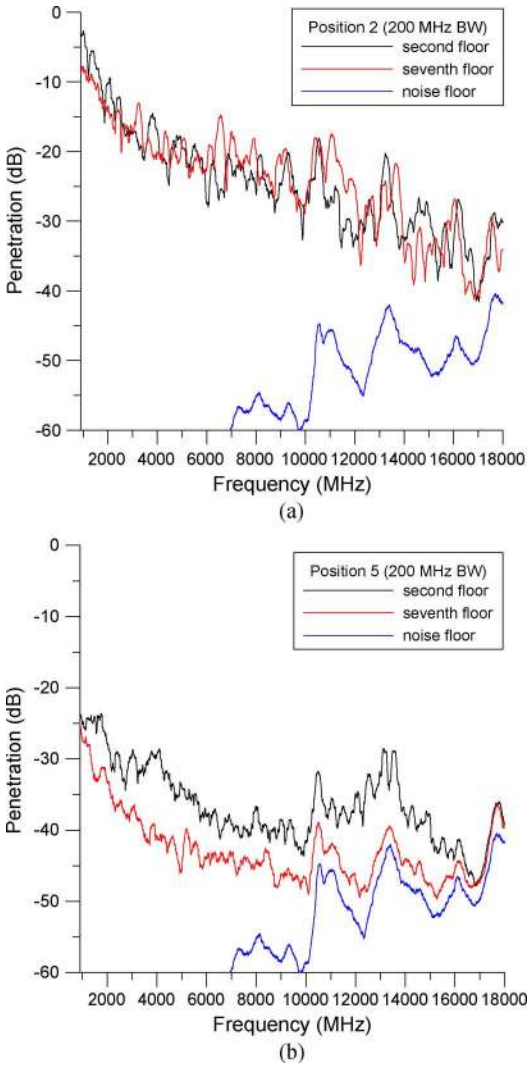

Fig. 6. Measured building penetration 1/(excess path loss), in dB, on Floor 2 (top, dark curves) and Floor 7 (middle, lighter curves) of the apartment building for frequencies from 1 GHz to 18 GHz at (a) position 2 and (b) position 5. The lower curves represent the noise floor of the VNA-based measurement system. Channel parameters such as loss and delay spread are calculated only where the signal is significantly in excess of the noise floor. A 200 MHz moving average filter has been applied to the data.

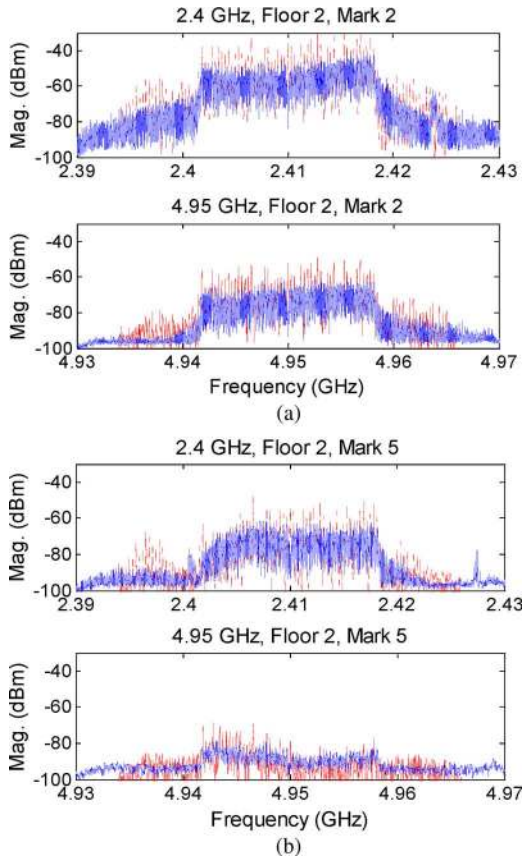

Fig. 7. Measured spectra across a 30 MHz bandwidth in the apartment building. (a) Test point 2, Floor 2; (b) test point 5, Floor 2. Top graphs for each location represent measurements for a carrier frequency of 2.4 GHz and bottom graphs for a carrier frequency of 4.95 GHz. Note that transmissions on other channels within the 2.4 GHz band are visible on the graphs.

through some type of building material. Building materials typically exhibit a monotonic increase in attenuation with frequency, changing on the order of decibels over several decades of frequency. The fact that the penetration curves (where the free-space path loss has been removed) in Fig. 6(a) measured on Floors 2 and 7 practically overlay indicates that the attenuation due to building penetration was similar on both floors. The difference in penetration between Floors 2 and 7 when the receiver is located behind the elevator indicates that more complicated, angle-dependent multipath scattering is involved in this propagation path.

Fig. 6 shows peaks and nulls that vary rapidly with frequency. These indicate multipath in the environment in addition to the building penetration effects. Because all of the received signal components arrive on non-line-of-sight paths, the phase relationship between them is random, indicating a Rayleigh distribution for the received signal. Note that the peaks and nulls that have structure (at higher frequencies) occur when the signal level approaches noise floor of the measurement system and do not give us information on the propagation channel. We neglect data whose level is not significantly in excess of the noise floor in our calculations of excess path loss and RMS delay spread.

Given that this is a multipath channel, it is useful to determine whether the multipath distortion is narrowband—where all frequency components in the modulation bandwidth are similarly affected by reflections, resulting in "flat" fading—or wideband—where peaks and nulls occur within the modulation bandwidth of the excitation, resulting in "frequency-selective" fading. Typically, wideband distortion is harder to overcome for radio receivers because different signal components are affected by the channel differently. Note that the definition of wideband distortion for a particular environment will be dependent on the excitation signal and the receiver used.

The VSA measurements exemplified in Figs. 7(a) and (b) indicate whether wideband distortion is present in the frequency band of interest. Here, we see the spectrum of the signal plotted versus frequency for the OFDM digitally modulated signal (dark curve) and for a multisine signal designed to simulate the RF statistics of the digitally modulated signal (lighter, dashed curve). The multisine is easier to generate and characterize using standard RF measurement instrumentation [30].

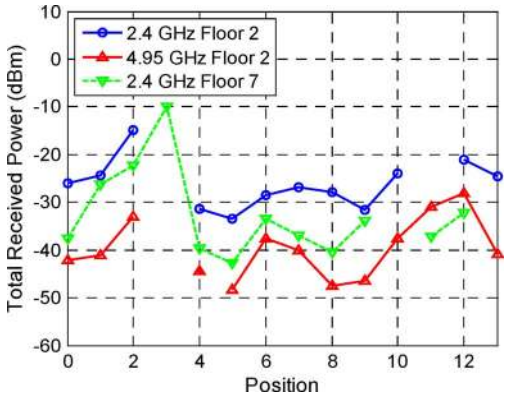

Fig. 8. Received power averaged across a 30 MHz bandwidth at 13 positions on two different floors of the 11-story apartment building for frequencies from 1 GHz to 18 GHz. Measurements were not recorded at all locations, as shown by the missing data points.

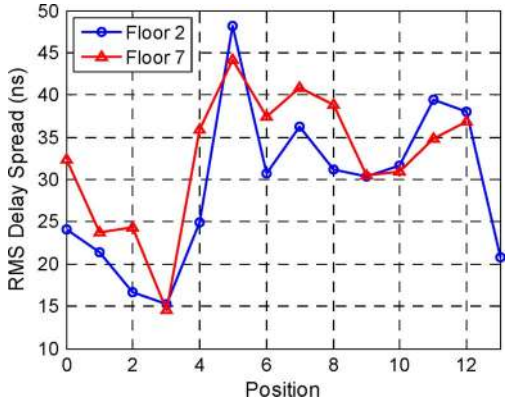

Fig. 9. RMS delay spread (ns) at 13 positions on two different floors of the 11-story apartment building made using a directional transmit antenna for frequencies between 1 GHz to 18 GHz.

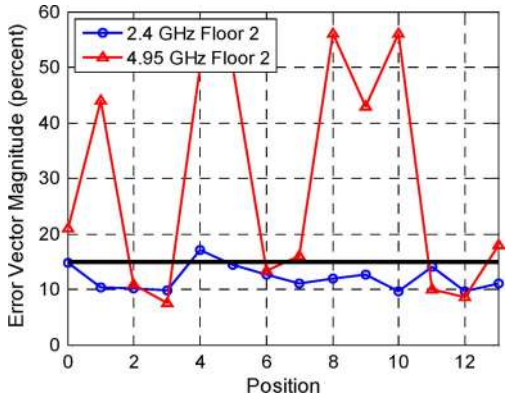

Fig. 10. EVM on Floor 2 of the apartment building for a QPSK-modulated OFDM signal for carrier frequencies of 2.4 GHz (circles) and 4.95 GHz (triangles). The thick black line represents an EVM of 15%. Measurements on Floor 7 were weak enough that it was difficult to determine the EVM.

The graphs in Fig. 7 show the received spectrum at test positions 2 and 5 on Floor 2. In each figure, the measurements in the top graph had a center frequency of 2.4 GHz and the bottom graph had a center frequency of 4.95 GHz. Note the additional signals received in the 2.4 GHz frequency band, both above and below the OFDM signal. These are from other 2.4 GHz wireless devices operating nearby. Emergency response organizations using unlicensed frequency bands may be susceptible to interference from other sources [17].

The VSA measurements show that the channel is generally frequency flat when simple building penetration through windows and concrete walls occurs; for example, at test position 2. However, frequency-selective distortion can be seen when the transmitter is behind the elevators or stairwell doors; for example, at test position 5.

A simple classification scheme for the propagation channels encountered in this type of building structure may be derived from the two frequency-domain measurements illustrated in Figs. 6 and 7. For the majority of the locations we tested, the channel could be classified as "simple building penetration," consisting of flat fading combined with decade-scale, frequency- and elevation-dependent path loss. The frequency and elevation dependence are indicated by the reduced overall signal level for the 4.95 GHz measurements, and for higher floors, respectively. In the location behind the elevator, we may classify the channel as "building penetration combined with frequency-selective fading." The latter, illustrated by the spectral variations shown in Fig. 7(b), is not the dominant channel classification in this type of building.

We next consider three summary metrics that can be used to derive the same classifications for the propagation channels as were derived from the frequency-domain representations above. Fig. 8 shows the received power of the OFDM signals averaged across a 30 MHz bandwidth. These graphs illustrate the frequency- and elevation-dependent path loss. When compared to the 2.4 GHz signal on Floor 2, the received power for the 4.95 GHz carrier frequency was on the order of 15 dB to 20 dB lower, and the received power for the 2.4 GHz carrier on Floor 7 was around 10 dB lower.

To classify the fading characteristics, we consider the RMS delay spread. Fig. 9 shows the RMS delay spread, computed for the entire high-frequency band, at all test positions on Floors 2 and 7. We see an increase in RMS delay spread when the receiver is blocked by the metallic elevator shaft, as expected. We see only a moderate increase in the RMS delay spread between the different floors, which is consistent with our classification of the majority of test positions as simple building penetration (attenuation as opposed to multipath).

The error vector magnitude plots shown in Fig. 10 illustrate a significantly lower EVM for the 2.4 GHz signal than for the 4.95 GHz signal. We see an increase in EVM at 2.4 GHz when the transmitter is shadowed by the elevator. Received signals whose EVM is high will have difficulty maintaining a link. An EVM of 15% is marked by the thick black line on the graph to denote channels that may be unusable. Because the dynamic range of the VSA is not as high that of the VNA-based measurement system, we were unable to obtain meaningful EVM measurements on Floor 7. However, we expect that the channel characteristics on Floor 7 are similar to those on Floor 2, based on the RMS delay spread measurements shown in Fig. 9.

The received power measurements again show a frequency and elevation dependence. RMS delay spread and EVM indicate that the multipath environment introduces both narrowband- and wideband-distortion. Whether we use the frequency measurements directly or a combination of summary metrics,

(a)

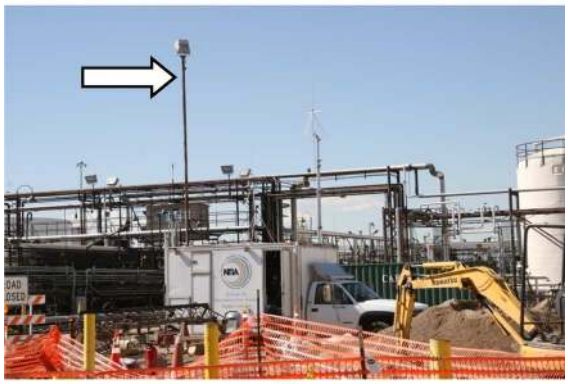

(b)

Fig. 11. Modulated-signal measurements made at an oil refinery: (a) transmitting unit consisting of a vector signal generator and omnidirectional antenna on a mobile cart inside dense piping in the facility. Photograph (b) shows the omnidirectional receiving antenna, indicated by an arrow, located on top of the ITS van.

analysis tells us we are dealing with a combination of simple building penetration in a multipath environment. This combination is representative of many similar structures where signals do not penetrate too deeply within a building.

C. Oil Refinery

A second example of the use of multiple metrics for propagation channel classification is illustrated by measurements conducted at a large oil refinery in Commerce City, Colorado in March 2007. As with the measurements at the apartment building, we chose this facility to simulate a response scenario (the Chemical Plant Explosion) in the SAFECOM Statement of Requirements [1].

The refinery is an outdoor facility covering many hectares in area, with intricate piping systems. We carried out tests primarily in an area of dense piping that forms a tunnel-like structure, shown in Fig. 11(a). We studied the propagation from a location outside the piping tunnel, shown in Fig. 11(b), to within the tunnel. Even though the site was outdoors, the dense piping was a significant barrier to radio communications and the propagation channel may be thought of as involving structure penetration.

Measurements were made at locations in the oil refinery indicated in Fig. 12 for both VNA and VSA measurements. One antenna (transmit antenna for the VNA measurements, receive

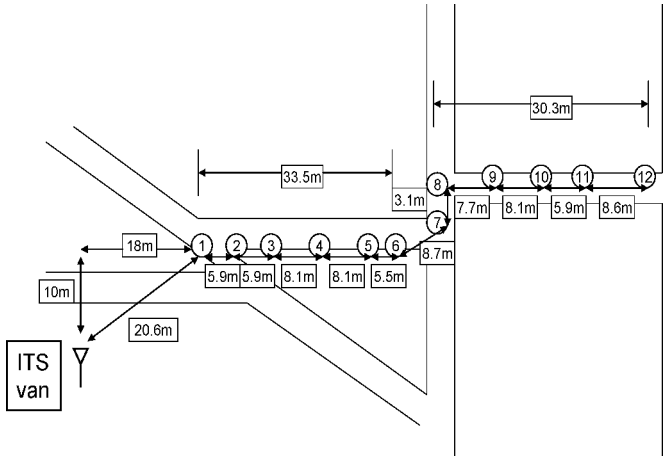

Fig. 12. Layout of the test positions for the excess path loss and modulated-signal measurements in the oil refinery complex. The test positions were located under dense overhead piping and metallic structures, in most cases several stories high.

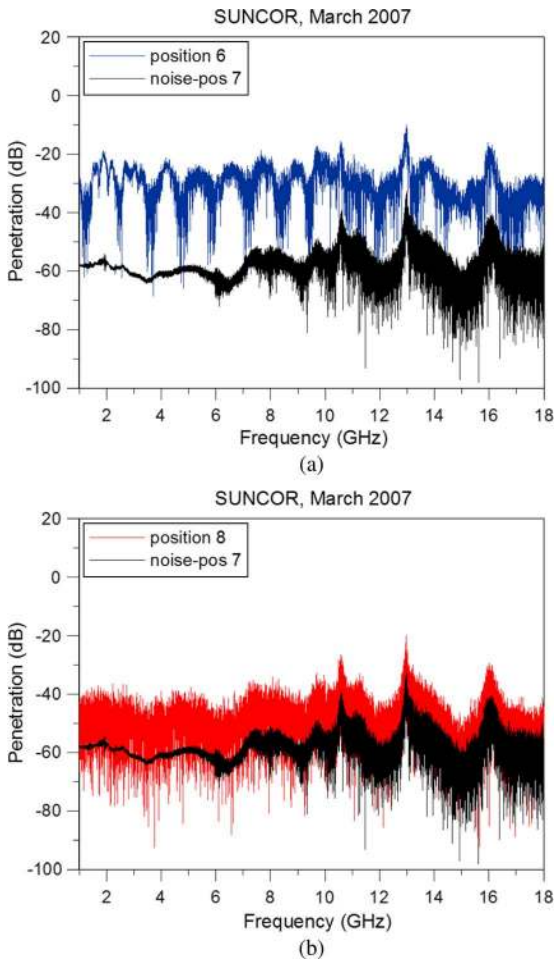

Fig. 13. Penetration 1/(excess path loss), in dB, measured at two locations in the oil refinery covering frequencies from 1 GHz to 18 GHz at (a) test position 6 (LOS) and (b) test position 8 (NLOS).

antenna for the VSA measurements) was located outside the piping complex on top of a mobile test van owned by the Institute for Telecommunication Sciences (ITS), a sister Department of Commerce organization at the Boulder Labs Site. This

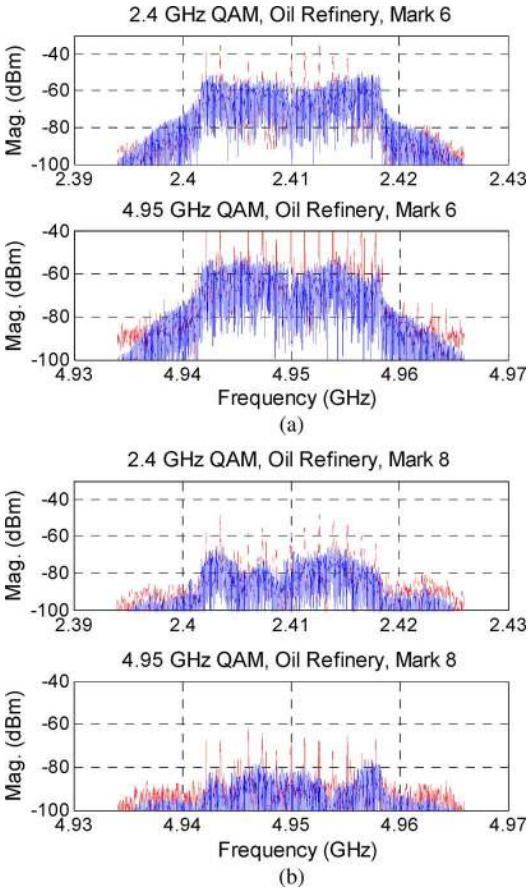

Fig. 14. Examples of the signal spectra derived from the VSA measurements of the modulated signal at (a) test position 6 and (b) test position 8 in the oil refinery. The top graphs represent measurements made at a carrier frequency of 2.4 GHz and the bottom graphs are for a carrier frequency of 4.95 GHz. These examples show 64QAM modulated signals.

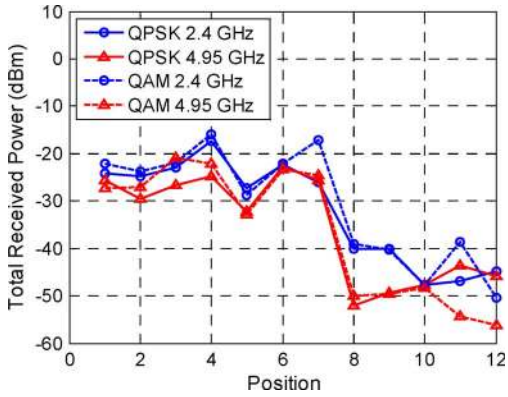

Fig. 15. Total received power averaged across a 30 MHz bandwidth for OFDM signals measured in the oil refinery for test positions 1 to 12.

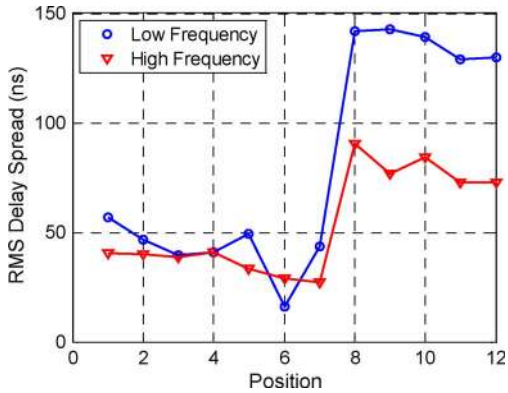

Fig. 16. RMS delay spread in the oil refinery at test positions 1 to 12. The curve with circles represents frequencies from 25 MHz to 1.2 GHz and the curve with inverted triangles represents frequencies from 1 GHz to 18 GHz.

antenna was vertically polarized. The photo in Fig. 11(b) shows the omnidirectional antenna mounted on the mast.

As may be expected, the many metallic surfaces in this environment introduced significant multipath into the signals we measured. Fig. 13 shows representative measurements of the penetration for frequencies from 1 GHz to 18 GHz.

Between test positions 2 and 6, the overhead piping created a tunnel-like environment where the multipath has significant structure. We see distinct frequency resonances at these positions, even though the receiving antenna had a line-of-sight condition with the transmitting antenna. Once the receiving antenna turned the corner, for test positions 7 and higher, no line-of-sight condition existed. The received signal took on a rapidly varying, Rayleigh, appearance.

We again consider the spectrum of the OFDM signal to assess the frequency-selective distortion in this environment. Representative VSA measurements are shown in Fig. 14. Our data showed only moderate frequency-selective distortion at test positions 2 to 6 (test position 6 is shown in Fig. 14(a)). This indicates that the extremely deep, frequency-resonant nulls in the penetration measurements of Fig. 13 are spaced widely enough that the modulated signal experiences multipath distortion that is flat across the bandwidth. Once the transmitter turns the corner, however, the signal experiences additional multipath that does introduce frequency-selective distortion, as shown in Fig. 14(b).

Based on the frequency-domain measurements above, the propagation channel in the oil refinery can be classified as "low attenuation, frequency flat" for the LOS conditions and "high attenuation, frequency-selective" for the NLOS conditions. We next study the use of the summary metrics total received power, RMS delay spread, and EVM to assess the same channel.

Fig. 15 shows the received power averaged across the modulation bandwidth of the OFDM signals. The signals with a carrier frequency of 4.95 GHz were approximately 5 dB to 10 dB lower than those with a carrier frequency of 2.4 GHz. When the receiver turned the corner into a NLOS condition, the received power levels dropped by around 15 dB for the 2.4 GHz signal and around 20 dB for the 4.95 GHz signal. Results were similar for both QPSK and 64QAM modulation formats, because the output power was the same for both transmissions.

A graph of the RMS delay spread in Fig. 16 shows short-duration values in the line of sight condition, and longer values after the receiver has turned the corner. The increase in delay spread is more significant for the low frequency band (100 MHz to 1.4 GHz) than for the high frequency band (1 GHz to 18 GHz).

The EVM graphs in Fig. 17 show that once the transmitter turns the corner, the EVM increases significantly. Before the turn, the EVM remains below 10% for both modulation formats.

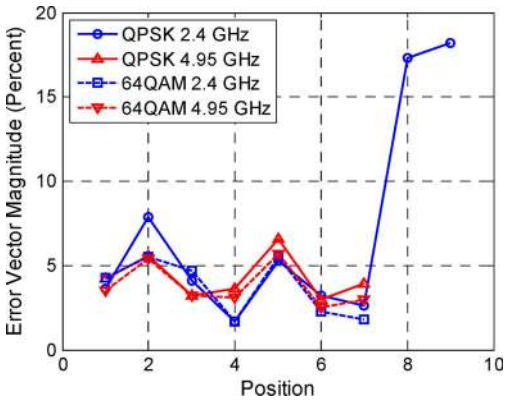

Fig. 17. EVM at the oil refinery for QPSK- and 64QAM-modulated OFDM signals for carrier frequencies of 2.4 GHz (circles and squares) and 4.95 GHz (triangles and inverted triangles.)

Even though significant multipath exists, this channel is probably usable.

Thus, using the frequency-domain metrics or the summary metrics, the oil refinery environment can be described as a channel that is low attenuation and flat fading under line-of-sight conditions, and high-attenuation with frequency-selective fading when in non-line-of-sight conditions. Additionally (not shown here), at the lower frequencies we saw attenuation due to lossy waveguide effects, where frequencies below the "cut-off" frequency of the tunnel were significantly attenuated [6], [31].

IV. Conclusion

We studied radio-wave propagation in representative environments of interest to the public-safety community. We used measurement configurations that replicate response scenarios, including point-to-point communications at human height, and receive sites located where response vehicles may be placed. Our study focused on measurements of quantities of interest in design, testing, and standards development for broadband, modulated-signal transmissions. These measurements included wideband penetration 1/(excess path-loss), in dB, measurements at specific locations in each structure and measurements of digitally modulated signals under the OFDM protocol at carrier frequencies of 2.4 GHz and 4.95 GHz. From the wideband path-loss measurements, we calculated channel power and RMS delay spread. From the modulated-signal measurements, we calculated error vector magnitude.

Here we reported on the results for an 11-story apartment building and an oil refinery. These tests show that a number of factors are needed to reliably define the propagation environment. Use of a combination of summary metrics such as received signal strength, RMS delay spread, and error vector magnitude can provide a fairly complete picture of the propagation environment, necessary for reliable deployment of radio systems, especially those employing wideband digital modulation. Because these summary measurements may be less expensive and complex to perform, use of summary metrics can save time and money.

In buildings where only one or two walls separate the transmit and receive antennas, such as the apartment building shown here, response organizations can expect to encounter simple building penetration with narrowband and, occasionally, wideband fading. These effects are expected to be common to environments that superficially appear quite different from each other. For certain propagation mechanisms such as simple building penetration, single-frequency signal-strength or channel power measurements may be sufficient to characterize the environment. In cases where multipath conditions exist, measurements that cover multiple frequencies and metrics such as RMS delay spread or EVM can offer additional insight.

It is clear that one critical factor for successful radio communications is knowledge of both the basic environmental characteristics (highly reflective, as in the industrial facility, or lossy building materials, such as windows and brick in the apartment building). A second factor is an understanding of the transmitted signal itself. If the signal is broadband, it is important to understand the sensitivity of the modulation format to flat- and frequency-selective multipath and attenuation. Finally, it is necessary to select the appropriate measurement metrics to be able to assess the environment for a given application. These procedures, as we have tried to illustrate here, are not difficult, but they do take some fore knowledge of the communication scenario. Consideration of these concepts will help to enable reliable communications for the public-safety community. Finally, we direct the reader to [5], [6] for data on other large structures.

References

[1] "SAFECOM Statement of Requirements," vol. 1, ver. 1.2 [Online]. Available:http://www.safecomprogram.gov/NR/rdonlyres/8930E37C-C672-48BA-8C1B-83784D855C1E/0/SoR1_v12_10182006.pdf, Section 3.3 and Section 3.5

[2] C. L. Holloway, G. Koepke, D. Camell, K. A. Remley, D. F. Williams, S. A. Schima, S. Canales, and D. T. Tamura, "Propagation and detection of radio signals before, during, and after the implosion of a 13-story apartment building," Nat. Inst. Stand. Tech. Note 1540, May 2005.

[3] C. L. Holloway, G. Koepke, D. Camell, K. A. Remley, D. F. Williams, S. A. Schima, S. Canales, and D. T. Tamura, "Propagation and detection of radio signals before, during, and after the implosion of a large sports stadium (Veterans' Stadium in Philadelphia)," Nat. Inst. Stand. Tech. Note 1541, Oct. 2005.

[4] C. L. Holloway, G. Koepke, D. Camell, K. A. Remley, S. A. Schima, M. McKinley, and R. T. Johnk, "Propagation and detection of radio signals before, during, and after the implosion of a large convention center," Nat. Inst. Stand. Tech. Note 1542, Jun. 2006.

[5] C. L. Holloway, W. F. Young, G. Koepke, K. A. Remley, D. Camell, and Y. Becquet, "Attenuation of radio wave signals coupled into twelve large building structures," Nat. Inst. Stand. Tech. Note 1545, Apr. 2008.

[6] K. A. Remley, G. Koepke, C. L. Holloway, C. Grosvenor, D. Camell, J. Ladbury, R. T. Johnk, D. Novotny, W. F. Young, G. Hough, M. D. McKinley, Y. Becquet, and J. Korsnes, "Measurements to support modulated-signal radio transmissions for the public-safety sector," Nat. Inst. Stand. Tech. Note 1546, Aug. 2008.

[7] [Online]. Available: http://www.nist.gov/eeel/electromagnetics/rf_fields/wireless.cfm

[8] [Online]. Available: http://www.antd.nist.gov/seamlessandsecure.shtml

[9] D. Molkdar, "Review on radio propagation into and within buildings," *Inst. Elect. Eng. Proc.-H*, vol. 38, no. 1, pp. 61–73, Feb. 1991.

[10] S. R. Sounders, K. Kelly, S. M. R. Jones, M. Dell-Anna, and T. J. Harrold, "The indoor-outdoor radio environment," *Inst. Elect. Eng. Elect. Comm. Eng. J.*, pp. 249–261, Dec. 2000.

[11] P. Papazian, "Basic transmission loss and delay spread measurements for frequencies between 430 and 5750 MHz," *IEEE Trans. Antennas Propag.*, vol. 53, no. 2, pp. 694–701, Feb. 2005.

[12] E. S. Sousa, V. M. Jovanovic, and C. Daigneault, "Delay spread measurements for the digital cellular channel in Toronto," *IEEE Trans. Veh. Tech.*, vol. 43, no. 4, pp. 837–847, Nov. 1994.
[13] G. Calcev *et al.*, "A wideband spatial channel model for system-wide simulations," *IEEE Trans. Veh. Tech.*, vol. 56, no. 2, pp. 389–403, Mar. 2007.
[14] J. R. Hampton, N. M. Merheb, W. L. Lain, D. E. Paunil, R. M. Shurfor, and W. T. Kasch, "Urban propagation measurements for ground based communication in the military UHF band," *IEEE Trans. Antennas Propag.*, vol. 54, no. 2, pp. 644–654, Feb. 2006.
[15] R. J. C. Bultitude, Y. L. C. de Jong, J. A. Pugh, S. Salous, and K. Khokhar, "Measurement and modeling of emergency vehicle-to-indoor radio channels and prediction of IEEE 802.16 performance for public safety applications," *IET Comm.*, vol. 2, no. 7, pp. 878–885, Aug. 2008.
[16] W. F. Young, C. L. Holloway, G. Koepke, D. Camell, Y. Becquet, and K. A. Remley, "Radio wave signal propagation into large building structures—Part 1: CW signal attenuation and variability," *IEEE Trans. Antennas Propag.*, vol. 58, no. 4, p. , Apr. 2010.
[17] T. L. Duomi, "Spectrum considerations for public safety in the United States," *IEEE Comm. Mag.*, vol. 44, no. 1, pp. 30–37, Jan. 2006.
[18] K. Balachandran, K. C. Budka, T. P. Chu, T. L. Duomi, and J. H. Kang, "Mobile responder communication networks for public safety," *IEEE Comm. Mag.*, vol. 44, no. 1, pp. 56–64, Jan. 2006.
[19] B. Davis, C. Grosvenor, R. T. Johnk, D. Novotny, J. Baker-Jarvis, and M. Janezic, "Complex permittivity of planar building materials measured with an ultra-wideband free-field antenna measurement system," *Nat. Inst. Stand. Technol. J. Res.*, vol. 112, no. 1, pp. 67–73, Jan.–Feb. 2007.
[20] M. Riback, J. Medbo, J. Berg, F. Harryson, and H. Asplund, "Carrier frequency effects on path loss," in *Proc. 63rd IEEE Vehic. Technol. Conf.*, 2006, vol. 6, pp. 2717–2721.
[21] K. A. Remley, G. Koepke, C. Grosvenor, R. T. Johnk, J. Ladbury, D. Camell, and J. Coder, NIST Tests of the wireless environment in automobile manufacturing facilities Nat. Inst. Stand. Tech. Note 1550, Oct. 2008.
[22] J. C.-I. Chuang, "The effects of time delay spread on portable radio communications channels with digital modulation," *IEEE J. Sel. Areas Comm.*, vol. SAC-5, no. 5, pp. 879–889, Jun. 1987.
[23] Y. Oda, R. Tsuchihashi, K. Tsuenekawa, and M. Hata, "Measured path loss and multipath propagation characteristics in UHF and microwave frequency bands for urban mobile communications," in *Proc. 53rd IEEE Vehic. Technol. Conf.*, May 2001, vol. 1, pp. 337–341.
[24] J. A. Wepman, J. R. Hoffman, and L. H. Loew, Impulse response measurements in the 1850–1990 MHz band in large outdoor cells NTIA Rep. 94-309, Jun. 1994.
[25] *IEEE Standard for Wireless LAN Medium Access Control (MAC) and Physical Layer (PHY) Specifications: High-Speed Physical Layer in the 5 GHz Band*, IEEE Standard 802.11a-1999.
[26] *IEEE Standard for Wireless LAN Medium Access Control (MAC) and Physical Layer (PHY) Specifications: Higher-Speed Physical Layer Extension in the 2.4 GHz Band*, IEEE Standard 802.11b-1999.
[27] M. D. McKinley, K. A. Remley, M. Myslinski, J. S. Kenney, D. Schreurs, and B. Nauwelaers, "EVM calculation for broadband modulated signals," in *64th ARFTG Conf. Dig.*, Orlando, FL, Dec. 2004, pp. 45–52.
[28] K. A. Remley, G. Koepke, C. L. Holloway, C. Grosvenor, D. G. Camell, and R. T. Johnk, "Radio communications for emergency responders in high-multipath outdoor environments," in *Proc. Int. Symp. Advanced Radio Tech.*, Boulder, CO, Jun. 2008, pp. 106–111.
[29] K. A. Remley, G. Koepke, C. L. Holloway, D. Camell, and C. Grosvenor, "Measurements in harsh RF propagation environments to support performance evaluation of wireless sensor networks," *Sensor Rev.*, vol. 29, no. 3, 2009.
[30] N. B. Carvalho, K. A. Remley, D. Schreurs, and K. G. Gard, "Multisine signals for wireless system test and design," *IEEE Microw. Mag.*, pp. 122–138, Jun. 2008.
[31] K. A. Remley, G. Hough, G. Koepke, D. Camell, C. Grosvenor, and R. T. Johnk, "Wireless communications in tunnels for urban search and rescue robots," in *Proc. Performance Metrics for Intelligent Systems Workshop (PerMIS)*, Aug. 2008, pp. 236–243, NIST Special Publication 1090.

Kate A. Remley (S'92–M'99–SM'06) was born in Ann Arbor, MI. She received the Ph.D. degree in electrical and computer engineering from Oregon State University, Corvallis, in 1999.

From 1983 to 1992, she was a Broadcast Engineer in Eugene, OR, serving as Chief Engineer of an AM/FM broadcast station from 1989–1991. In 1999, she joined the Electromagnetics Division, National Institute of Standards and Technology (NIST), Boulder, CO, as an Electronics Engineer. Her research activities include metrology for wireless systems, characterizing the link between nonlinear circuits and system performance, and developing methods for improved radio communications for the public-safety community.

Dr. Remley was the recipient of the Department of Commerce Bronze and Silver Medals and an ARFTG Best Paper Award. She is currently the Editor-in-Chief of *IEEE Microwave Magazine* and Chair of the MTT-11 Technical Committee on Microwave Measurements.

Galen Koepke (M'94) received the B.S.E.E. degree from the University of Nebraska, Lincoln, in 1973 and the M.S.E.E. degree from the University of Colorado at Boulder, in 1981.

He is an NARTE Certified EMC Engineer. He has contributed, over the years, to a wide range of electromagnetic issues. These include measurements and research looking at emissions, immunity, electromagnetic shielding, probe development, antenna and probe calibrations, and generating standard electric and magnetic fields. Much of this work has focused on TEM cell, anechoic chamber, open-area-test-site (OATS), and reverberation chamber measurement techniques along with a portion devoted to instrumentation software and probe development. He now serves as Project Leader for the Field Parameters and EMC Applications program in the Radio-Frequency Fields Group. The goals of this program are to develop standards and measurement techniques for radiated electromagnetic fields and to apply statistical techniques to complex electromagnetic environments and measurement situations. A cornerstone of this program has been National Institute of Standards and Technology (NIST), work in complex cavities such as the reverberation chamber, aircraft compartments, etc.

Christopher L. Holloway (S'86–M'92–SM'04–F'10) was born in Chattanooga, TN, on March 26, 1962. He received the B.S. degree from the University of Tennessee at Chattanooga in 1986, and the M.S. and Ph.D. degrees from the University of Colorado at Boulder, in 1988 and 1992, respectively, both in electrical engineering.

During 1992, he was a Research Scientist with Electro Magnetic Applications, Inc., Lakewood, CO. His responsibilities included theoretical analysis and finite-difference time-domain modeling of various electromagnetic problems. From fall 1992 to 1994, he was with the National Center for Atmospheric Research (NCAR), Boulder. While at NCAR his duties included wave propagation modeling, signal processing studies, and radar systems design. From 1994 to 2000, he was with the Institute for Telecommunication Sciences (ITS), U.S. Department of Commerce in Boulder, where he was involved in wave propagation studies. Since 2000, he has been with the National Institute of Standards and Technology (NIST), Boulder, CO, where he works on electromagnetic theory. He is also on the Graduate Faculty at the University of Colorado at Boulder.

Dr. Holloway was awarded the 2008 IEEE EMC Society Richard R. Stoddart Award, the 2006 Department of Commerce Bronze Medal for his work on radio wave propagation, the 1999 Department of Commerce Silver Medal for his work in electromagnetic theory, and the 1998 Department of Commerce Bronze Medal for his work on printed circuit boards. His research interests include electromagnetic field theory, wave propagation, guided wave structures, remote sensing, numerical methods, and EMC/EMI issues. He is currently serving as Co-Chair for Commission A of the International Union of Radio Science and is an Associate Editor for the IEEE TRANSACTIONS ON ELECTROMAGNETIC COMPATIBILITY. He was the Chairman for the Technical Committee on Computational Electromagnetics (TC-9) of the IEEE Electromagnetic Compatibility

Society from 2000–2005, served as an IEEE Distinguished lecturer for the EMC Society from 2004–2006, and is currently serving as Co-Chair for the Technical Committee on Nano-Technology and Advanced Materials (TC-11) of the IEEE EMC Society.

Chriss A. Grosvenor (M'91) was born in Denver, CO. She received the B.A. degree in physics and M.S. degree in electrical engineering from the University of Colorado, Boulder, in 1989 and 1991, respectively.

In 1990, she joined the Electronics and Electrical Engineering Laboratory, National Institute of Standards and Technology (NIST), Boulder, CO. Her work at NIST includes design and analysis of large stripline cavities for materials measurements as well as a large 77 mm diameter coaxial system and a 60 GHz Fabry-Perot resonator. She has worked in the noise temperature project and assembled the 1 to 12 GHz automated systems and repackaged the 30 and 60 MHz noise temperature measurement systems. She joined the time-domain project in 2002 and has worked on measurements of shielding effectiveness of aircraft including the orbiter Endeavour. She has authored papers in all of these technical areas.

Ms. Grosvenor was awarded the Bronze Medal for her work with the orbiter Endeavour.

Dennis Camell (M'94) received the B.S. and M.E. degrees in electrical engineering from the University of Colorado, Boulder, in 1982 and 1994, respectively.

From 1982 to 1984, he worked for the Instrumentation Directorate, White Sands Missile Range, NM. Since 1984, he has worked on probe calibrations and EMI/EMC measurements with the Electromagnetics Division, National Institute of Standards and Technology (NIST), Boulder, CO. His current interests are measurement analysis (including uncertainties) in various environments, such as OATS and anechoic chamber, and development of time domain techniques for use in EMC measurements and EMC standards. He is involved with several EMC working standards committees and is chair of ANSI ASC C63 SC1.

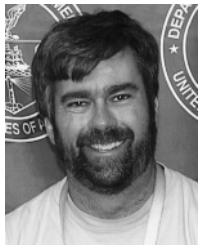

John Ladbury (M'92) was born Denver, CO, 1965. He received the B.S.E.E. and M.S.E.E. degrees in signal processing from the University of Colorado, Boulder, in 1987 and 1992, respectively.

Since 1987 he has worked on EMC metrology and facilities with the Radio Frequency Technology Division, National Institute of Standards and Technology (NIST), Boulder, CO. His principal focus has been on reverberation chambers, with some investigations into other EMC-related topics such as time-domain measurements and probe calibrations. He was involved with the revision of RTCA DO160D and is a member of the IEC joint task force on reverberation chambers.

Mr. Ladbury has received three "best paper" awards at IEEE International EMC symposia over the last six years.

Robert T. Johnk, photograph and biography not available at the time of publication.

William F. Young (M'06) received the B.S. degree in electronic engineering technology from Central Washington University, Ellensburg, in 1992, the M.S. degree in electrical engineering from Washington State University at Pullman, in 1998, and the Ph.D. degree from the University of Colorado at Boulder, in 2006.

Since 1998, he has worked for Sandia National Laboratories in Albuquerque, NM, where he is currently a Principal Member of the Technical Staff. His work at Sandia includes the analysis and design of cyber security mechanisms for both wired and wireless communication systems used in the National Infrastructure and the Department of Defense. He has also been a Guest Researcher at the National Institute of Standards and Technology in Boulder, CO, from 2003 to 2009, and is working on improving wireless communication systems for emergency responders. His current research interests are in electromagnetic propagation for wireless systems, and the impacts of the wireless channel on overall communication network behavior.